

Active Constraints in robot-assisted minimally invasive surgery

Nicolò Pasini

Person Code: 10576999

Student Number: 971406

nicolo1.pasini@mail.polimi.it

Matteo Pecorella

Person Code: 10755787

Student Number: 967727

matteo.pecorella@mail.polimi.it

Alberto Rota

Person Code: 10615751

Student Number: 964662

alberto2.rota@mail.polimi.it

Abstract—Active constraints are control strategies used in robotic surgery that restrict or adjust the the motion of the surgical tool with respect to predefined paths, trajectories, surfaces and volumes, often disregarding the commands from the controller. This paper presents the application of a specific guidance active constraint, which aims at piloting the operator in following a predefined path in a surgical scenario by applying a viscous feedback force on the hand-held manipulator of the master controller. The study has been conducted on a *daVinci* Surgical Robot and in a Unity virtual scene.

Index Terms—Robotic surgery, active constraints, trajectory guidance, force-feedback

I. INTRODUCTION

Fully autonomous robotic systems are currently used in many varied applications. They can offer many advantages over humans, such as superior accuracy and precision. There are, although, also limits to their abilities, for example to perceive and evaluate highly unstructured environments, due also to data processing limitations and limited knowledge base concerning the task. Humans, instead, are particularly adept at dealing with this type of situations. By using a robot to intelligently regulate the motion of a human user, rather than replace the human entirely, many of the challenges above can be overcome by also keeping the advantages of using a robot (*Figure1*).

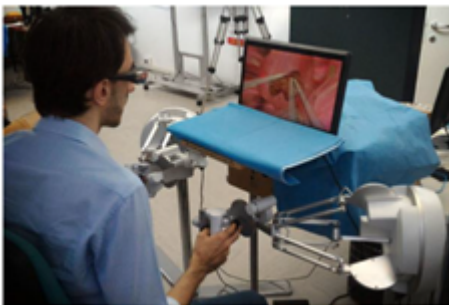


Fig. 1. Example of human/robot integration

In this context the “active constraints” (or “virtual fixtures”), are defined. They are collaborative control strategies, which can be used to improve or assist human manipulation tasks [1], with a motion regulation performed by attaching tools to a robotic arm, which is primarily controlled by the human user. Throughout operation, the robot controller monitors the

tool motion with respect to predefined trajectories or restricted regions. The active constraint controller then attenuates or nullifies any user command, which will cause the manipulator to digress from the plan or enter the restricted region.

There are many different active constraints strategies depending on some characteristics, for example Regional or Guidance active constraints, Attractive or Repulsive, Unilateral or Bilateral [1]; the combination of these characteristic is chosen depending on the application.

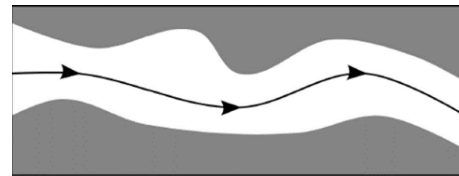


Fig. 2. Example of a guidance active constraint

The aim of this work is to create a Guidance active constraint (as in *Figure 2*), to make a human operator to follow a predefined trajectory, to protect organs in robot assisted minimally invasive surgery performed with a *Da Vinci* machine. This algorithm implements a viscosity-based dynamic guidance constraint that continuously redirects the *Da Vinci* tool's motion towards the reference path. A viscosity-based guidance constraints relies on the concept of viscosity to compute the force that the robot applies on the tool controlled by the human operator. In particular, the faster and the more the tool moves away from the desired trajectory, the bigger the force magnitude will be. The proportionality and continuity of generated forces make the method not much distracting and subjectively appealing.

In the following paragraphs it is explained more in detail the different parts of the project such as the virtual environment simulation in Unity, the viscosity force computation formulas, and the actual implementation of the active constraints on the *Da Vinci Surgical Kit* (DVRK).

II. MATERIALS AND METHODS

Studies and implementations of this specific application of virtual fixtures have been conducted at first on a simulated environment, which allowed for a higher flexibility in the development and for a risk-free testing phase. A virtual operating room has been set up in a Unity scene, comprehensive

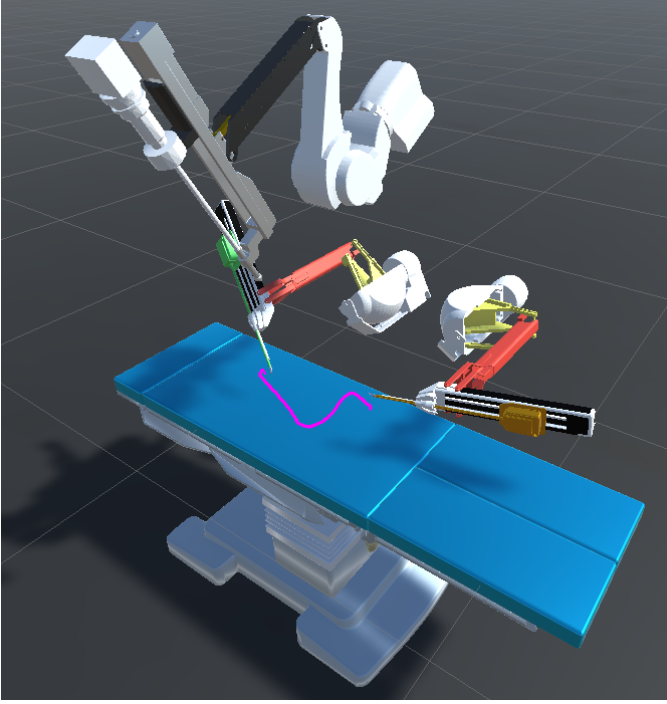


Fig. 3. Unity Virtual Environment, with two PSMs, one ECM, the path (in magenta) and the operating table.

of an operating table, two Patient-Side Manipulators (PSMs) and one Endoscope Camera Manipulator (ECM), as shown in *Figure 3*. The actuation commands received from the Master Tool Manipulators (MTMs) at the control station are sent to the Unity environment through a ROS framework, which will also be the basis for the force feedback communication once the force vector is computed. Therefore, the motion from the operator on the MTMs is translated into the motion of both the end-effector of the PSMs and of the 3D model in the Unity scene. This approach allows to position a pre-defined path in the virtual environment, representing the desired trajectory of the surgical tool: the end-effector position in the real environment is mimicked by the one in the virtual simulation, which is used to calculate the force feedback of the active constraint based on the relative positioning of the end-effector and the path.

The feedback force computed for the virtual fixture is of viscous type, as its magnitude depends on the velocity of the end-effector in space: a more detailed discussion on this kind of active constraint is given in [2]. The force magnitude f at each time step is, in this case, calculated as:

$$f = \begin{cases} b \cdot \|\mathbf{v}\| & \text{if } f < f_{max} \\ f_{max} & \text{if } f \geq f_{max} \end{cases} \quad (1)$$

\mathbf{v} is the velocity vector of the end-effector in space and b is an anisotropic coefficient obtained as follows:

$$b = B \cdot \sqrt{\frac{1 - \hat{\mathbf{v}} \cdot \hat{\mathbf{d}}}{2}} \quad (2)$$

Here \mathbf{d} is the *deviation*, denoted as the vector going from the end-effector to the closest point in the path, while B represents the maximum value of the viscosity coefficient and it is set by the operator. Equation 2 makes sure that the coefficient b is maximum when the velocity is opposite to the deviation (occurring when $\hat{\mathbf{v}} \cdot \hat{\mathbf{d}} = -1$) and minimum when the two vectors are aligned ($\hat{\mathbf{v}} \cdot \hat{\mathbf{d}} = 1$).

The force direction $\hat{\mathbf{f}}$ is computed as:

$$\hat{\mathbf{f}} = \begin{cases} \hat{\mathbf{d}} & \text{if } \hat{\mathbf{v}} \cdot \hat{\mathbf{d}} < 0 \\ \text{rotate}(\hat{\mathbf{v}}, \theta, \mathbf{n}) & \text{otherwise} \end{cases} \quad (3)$$

where the $\text{rotate}(\cdot)$ function rotates the velocity vector $\hat{\mathbf{v}}$ around the axis denoted by vector \mathbf{n} of θ degrees. Equation 3 is built so that, if the end-effector is moving away from the path (a condition occurring when the dot product between $\hat{\mathbf{v}}$ and $\hat{\mathbf{d}}$ is negative), the force direction is aligned with the deviation direction, granting therefore independence from the direction of velocity. Conversely, the vector rotation is applied solely in the cases where the end-effector approaches the path, and in this case the angle and axis of rotation are defined as:

$$\theta = (1 + \hat{\mathbf{v}} \cdot \hat{\mathbf{d}}) \cdot \frac{\pi}{2} \quad (4)$$

$$\mathbf{n} = \hat{\mathbf{v}} \times \hat{\mathbf{d}} \quad (5)$$

Finally, the constraint force \mathbf{f} is found from the scalar multiplication

$$\mathbf{f} = f \cdot \hat{\mathbf{f}} \quad (6)$$

The computation happens in real time during the operation, and a force vector is hence available at any timestamp and is communicated to the master controller of the DVRK on a ROS topic.

The ROS framework is essential and covers the whole communication network between the master controller, the surgical robotic arms and the virtual environment. For this specific purpose, the relevant ROS communications are:

- The *Joint state* messages published by the PSMs and subscribed by the Unity scene, which allow the replication of the motion of the real robotic arm by the virtual 3D models
- The *Wrench* message published by the Unity virtual environment and subscribed by the MTMs, containing the force feedback vector
- The *gravity compensation* message, which allows to account for the effect of gravity when applying the force on the MTMs.

The force obtained above in Equation 6 is sent, as a ROS *Twist* object, on the *Wrench* topic which is subscribed by the master controller.

TO DO: ADD HERE AFTER THE NEXT LAB MEETING

III. RESULTS

After the implementation of the methods described above, we collected data coming from the simulation both for force, velocity and deviation estimation. As depicted in *Figure 4*, it's

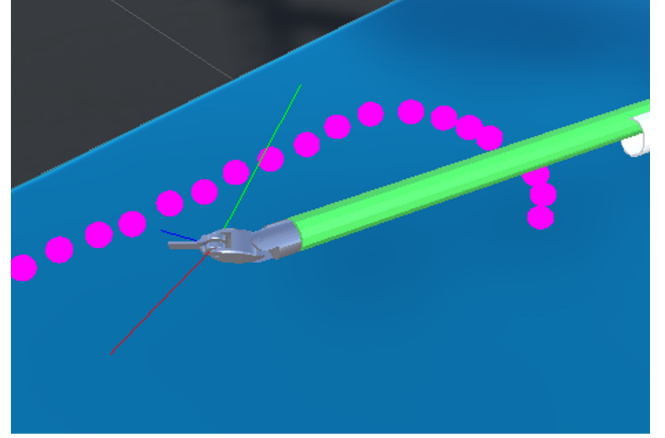
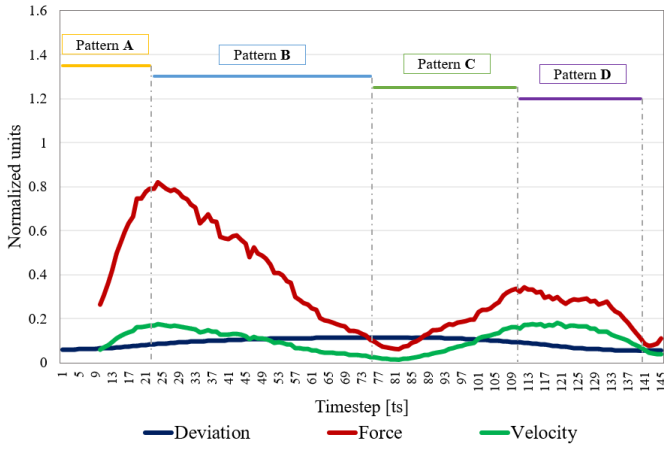


Fig. 4. *Left*: Magnitude of the force, deviation and velocity vectors during movements distancing (Patterns A and B) and approaching (Patterns C and D) the predefined path. *Right*: Visualization of the three vectors as applied on the surgical tool. In magenta, samples from the planned trajectory.

clear that there exists a trend followed by every single plotted feature.

Please notice that, since the three variables are grouped together, on the y-axis no unit of measurement is specified, while on the common x-axis we can find the timestamps, according to the DVRK acquisition frequency (????). Furthermore, due to an intrinsic instability in the virtual models, both for PSMs and ECM, the extracted force, velocity and normal (not shown, for sake of simplicity) values needed to be filtered. As we can see from the plots evaluation, the initial raw data are characterized by an inconvenient noise, which is the origin of those unreadable spikes and downs. In order to manage the trembling effects, we applied a moving average, with time period = 18 timestamps [ts], and overlapped the results to the original raw data, for a better understanding. This is the reason why only deviation, the blue line, starts without lagging: force (red) and velocity (green) start from $ts=9$, which is the mid-point for the first 18 averaged timestamps. Furthermore, the magnitude of all three variables clearly do not hold any information regarding the orientation of such vectors: for the purpose of the work, the following discussion is considered to be elucidative enough without decomposing each vector into its three components, along the cartesian axes, since the direction of each vector can be deduced from the trend of the other two.

IV. DISCUSSION

The data acquisition process starts as soon as the MTMs are enabled for user control [$ts=1$]. The first increasing trend, around $ts=43$, describes the first movement applied to the tool tip: an increase in deviation means the user was pulling the tool away from the original path, until $ts=103$. During this first phase, both force and velocity have a parabolic behaviour: this is due to the starting and ending velocity being equal to zero. In fact, force always follows velocity: while moving far away from the path the computed force tends to redirect the user in the opposite direction, towards the nearest point, and its

magnitude will increase as long as both velocity and deviation increase too. Around $ts=70$ there's an inversion in the trend: this is due to the decrease in velocity, even if the tool tip is still moving away from the path, hence deviation is still increasing. The descending phase of the deviation [from $ts=103$ to $ts=157$] is as elucidative as the ascending one: as described before, force still follows velocity, but its increase in magnitude is halved even if velocity reaches higher values. This behaviour can be explained again referring to the expressions 1 to 6.

Force computation takes into account both the velocity magnitude and direction, and it can be seen analysing the force's parabolic trends with respect to the deviation derivative, in these four particular patterns repeated multiple times in *Figure 4*.

Pattern A Increasing deviation and velocity: the tool tip is moving away from the path, both the variables have a positive contribute in the increase of force magnitude. Force and velocity increase till they both reach local maxima when deviation's derivative reaches its peak.

Pattern B Increasing deviation, decreasing velocity: the tool tip is still moving away from the path, but is decelerating, hence deviation is the only positive contribute. Force starts decreasing and follows velocity's trend till they both reach local minima when deviation's derivative is zero: the tool tip is temporary still.

Pattern C Decreasing deviation, increasing velocity: the tool tip has reversed course and started approaching the path at an increasing velocity, which is the main positive contribute to the computations. Force starts increasing again, but the decreasing deviation tends to lower its magnitude, resulting in a parabolic trend, as for the ascending part, with reduced values. Peaks reached inside this pattern are the lowest local maxima encountered during experiments.

Pattern D Decreasing deviation, decreasing velocity: the tool tip has almost reached the path, so the user decreases its velocity. Both deviation and velocity have a negative contribute to force's magnitude, which reaches again a local minimum.

Which one of these two?

— The local minima, both for velocity and force are reached when the deviation derivative is zero, hence no difference is noted among the minima related to approaching and distancing movements

— Since the local minima, both for velocity and force, are reached when the deviation derivative is zero, no differences will be noted between them, as they all fall around zero.

The described pattern can be seen repeated two times in *Figure 4*: please, follow notations inside the plot for a better understanding.

V. CONCLUSIONS

REFERENCES

- [1] Stuart A Bowyer, Brian L Davies, and Ferdinando Rodriguez y Baena. Active constraints/virtual fixtures: A survey. *IEEE Transactions on Robotics*, 30(1):138–157, 2013.
- [2] Nima Enayati, Eva C. Alves Costa, Giancarlo Ferrigno, and Elena De Momi. A dynamic non-energy-storing guidance constraint with motion redirection for robot-assisted surgery. In *2016 IEEE/RSJ International Conference on Intelligent Robots and Systems (IROS)*, pages 4311–4316, 2016.